European Conference on Computational Fluid Dynamics
ECCOMAS CFD 2006
P. Wesseling, E. Oñate, J. Périaux (Eds)

STATUS OF WAKE VORTEX ALLEVIATION IN THE FRAMEWORK OF EUROPEAN COLLABORATION: VALIDATION ATTEMPTS USING TESTS AND CFD RESULTS

Eric COUSTOLS*, Laurent JACQUIN† and Geza SCHRAUF‡

* ONERA/DMAE, Aerodynamics and Energetics Modelling Department,
B.P. 4025, 2 Avenue Edouard Belin, 31055 Toulouse Cedex, France.
e-mail: Eric.Coustols@onera.fr ; Web page: http://www.onera.fr/dmae-en/index.php

† ONERA/DAFE, Fundamental and Aerodynamics Department,
8 rue des Vertugadins, 92190 Meudon, France.
e-mail: Laurent.Jacquin@onera.fr ; Web page: http://www.onera.fr/dafe-en/index.php

‡ Airbus Deutschland GmbH, EGAG,
Huenefeldstr. 1-5, 28183 Bremen, Germany.
e-mail: Geza.Schrauf@airbus.com ; Web page: http://www.airbus.com

Key words: Wake Vortex, Wind Tunnel, Towing Tank, Catapult, Alleviation, Passive and Active Control, Device, Differential Span Loading.

Abstract. *This document provides a synthesis of recent research studies that have been conducted in the last decade within several European projects from the 5th and 6th Framework Programmes. All these studies aimed at a better characterization of aircraft wake vortices and then at their subsequent control. In the latter case, the goal is to minimize the strength of such vortices in the far-field. At first, characterisation of wake vortex using complementary tools (testing facilities, flight tests, simulations and theory) will be briefly evoked. Secondly, information will be provided on the main principles for wake vortex alleviation. At last, results and then recommendations will be detailed from the considered practical approaches.*

1 INTRODUCTION

Research on Wake Vortex Alleviation has been conducted in the last decade within the framework of European partnership, notably as part of programmes sponsored by the European Commission like Eurowake, C-Wake, AWIATOR or, more recently, Far-Wake (Figure 1). Thus, important experimental as well as numerical data have been generated by several partners, using complementary approaches: on the theoretical side from analytical models up to sophisticated numerical methods and experimentally from sub-scale tests in wind tunnel, towing tank or catapult facilities up to full-scale flight trials (each requiring the development of appropriate instrumentation). Results from such trials will not be covered in the present paper; information can be found in [17,18,23].

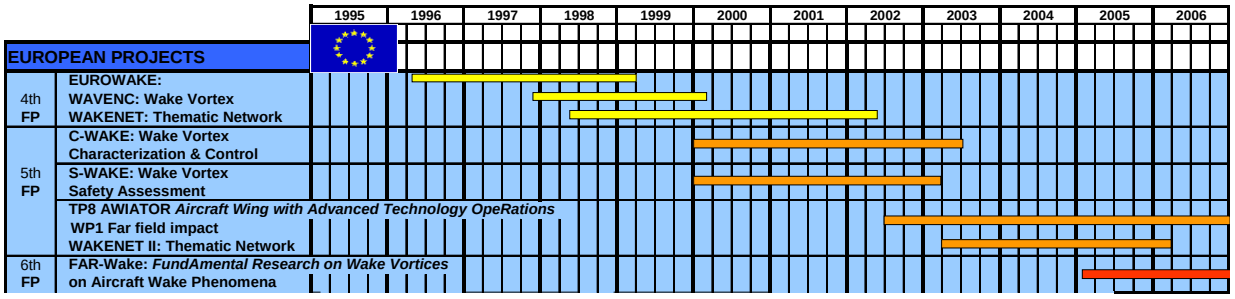

Figure 1 – Wake vortex studies/projects in the framework of European partnership [33].

The present paper aims at illustrating main results in the field of wake vortex alleviation, recorded from dedicated testing campaigns. Specific care has been devoted to the generation of such data bases, since these latter will be used for validation of complementary CFD tools.

The two main strategies, applied for wake vortex minimisation in the framework of the above-cited European projects, will be developed; results on "what has been achieved so far" are also discussed in detail. But, at first, some physical background of aircraft wake vortices will be briefly recalled, as well as some general discussions on experimental and numerical tools most appropriate for wake vortex characterisation and control.

2 WAKE VORTEX FLOW: CHARACTERISATION AND CONTROL

2.1 Background

The lift force generated by an aircraft wing produces generally two counter-rotating vortices that can persist for long times. The basic physics of such a single vortex pair wake is reasonably well understood. When the vortex is generated, its strength Γ_0 follows:

$$\Gamma_0 = \frac{W}{\rho U b s} = \tfrac{1}{2}\frac{C_L U b}{ARs} \qquad t_0 = \frac{2\pi\rho U (bs)^3}{W} = \frac{4\pi ARbs^3}{C_L U} \tag{1}$$

with W, b, AR and C_L the weight, wing span, wing aspect ratio and lift coefficient of the aircraft, respectively. U and ρ are the aircraft speed and air density. s is a dimensionless parameter defined by the distance between the vortices divided by the wing span b; s depends on the wing loading and is equal to $\pi/4$ for an elliptical lift distribution.

As soon as the vortices have formed, they will move downwards (due to their mutual induction) and decay. The evolution of the wake vortex behind an aircraft is very often described versus either its distance x to the aircraft, normalised by the aircraft wing span b, ($x^*=x/b$), or by a non-dimensional time τ^* ($=t/t_0$). Here t_0 is the time in which a vortex pair propagates the distance of one initial vortex spacing downwards and thus equal to b_0/w_0, where b_0 ($=b.s$) is the initial vortex spacing and w_0 the initial sink speed [10,28]. The larger the value of t_0 [cf. Equation (1) for the expression of t_0 in terms of aircraft parameters] the slower the vortex decays. These scaling rules are (believed to be) known, although it has to be

noted that there is in fact no “full size” proof of the τ^* scaling (too much scatter in the "in flight" data sets to discriminate between aircraft of different sizes).

During their evolution, the vortices grow in size, due to diffusion and develop oscillations caused by flow instabilities that may lead to strong interactions between the vortices and increased dissipation. During the 1st stage of the decay, as long as the two vortices stay apart from each other, the vortex circulation Γ and the vortex spacing b_0 are essentially constant. Only in the later stages, when the two vortices interact, Γ will decrease and b_0 will increase. To express the intensity of the vortex the circulation, various quantities can be used:

- $\Gamma_{5\text{-}15}$, the averaged circulation between 5 and 15m distance to the vortex core, from Lidar measurements for real aircraft applications, but usually considered to the integral between *b/12* and *b/4* for aircraft models,
- E_{kin} the cross-flow kinetic energy (initial value being related to the induced drag),
- the core radius r_c (distance of the vortex centre to the maximum tangential velocity),
- the maximum tangential (or peak) velocity $V_{t,max}$ at the core radius r_c.

For a particular profile family of the tangential velocity, these 4 quantities can be directly related to each other [9]. Due to diffusion of vorticity, $\Gamma_{5\text{-}15}$, E_{kin} and $V_{t,max}$ decrease downstream whereas r_c increases.

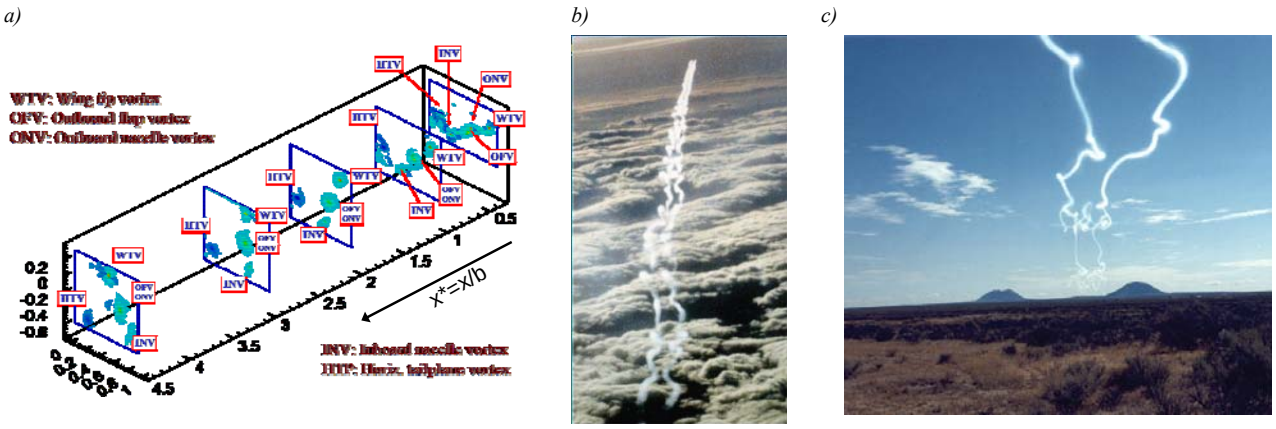

Figure 2 – Illustrations of wake flow fields a) Regions I & II: iso-contours of vorticity behind high-lift configurations (AWIATOR, exp. performed by TUM-AER [32]); b) & c) Regions III to IV (from [40]).

The vortex field behind the aircraft is then generally split in four regions (Figure 2):

- the near-wake field (**Region I**, typically of the order of the chord length *c*) very close to the wing trailing edge, which comprises vortex sheets and highly concentrated vortices;
- the extended near-wake field (**Region II**, typically $0.5<x^*<10\text{-}15$, or $0.25<\tau^*<0.5$) in which the roll-up and merging of the vortex sheet and the vortices occur, in most cases leading to two main counter-rotating vortices;
- the mid-wake field (**Region III**, at a maximum distance $x^*\sim100$ or $\tau^*\sim2.5$) where the vortex system gradually drifts downwards due to mutual interaction of the vortices and where the instabilities emerge;

- at last, the far-wake field (**Region IV**, $x^*>100$ or $\tau^*>\sim 2.5$) where developed instabilities result in strong interactions between these two main vortices leading to their dispersal.

Note that the given values are for quiet air. For other weather conditions with turbulence, shear or inversions these values can be considerably less.

2.2 Experimental techniques: ground facilities

The wake vortex formation, as well as the roll-up phase, is reasonably well understood since many investigations have been conducted in standard facilities (wind tunnels), with appropriate measurement tools [3,8,20,21]. In the mid- to far-wake field, the towing tank and the free-flight (catapult) facility are the only tools which allow such wake flow scrutinising (Fig. 3). In the framework of the C-Wake project, several tests conducted in the towing tank and catapult facility showed anomalies that could be understood from boundary or installation effects (known as end-effects) and temperature stratification [8]. Specific new test campaigns have been performed in the AWIATOR project, during which these effects were carefully investigated and cross-checks were made for these two specific facilities [3,24].

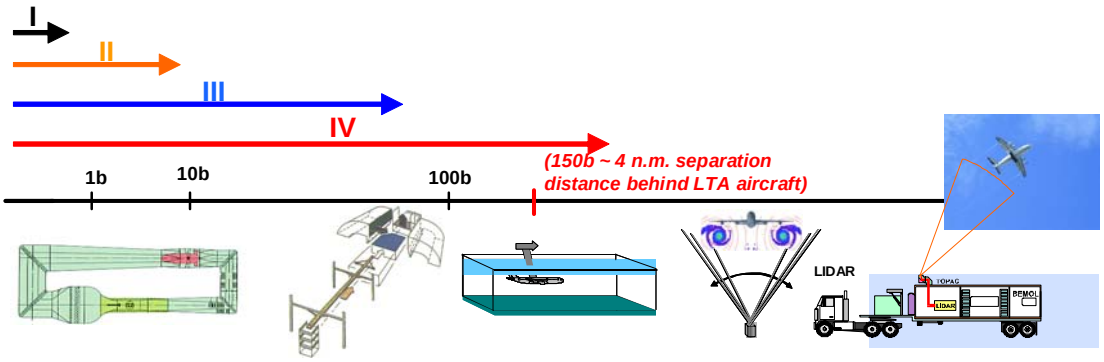

Figure 3 – Four regions of the wake flow field as well as their dedicated facilities for investigations [3,33].

End-effects were carefully monitored and observed by Airbus-Deutschland, DLR and ONERA during some dedicated tests; UCL conducted also investigations at the UCL/TERM towing tank [11]. They are the result of instabilities (axial-type travelling waves) that move up- and downstream through the vortex core and that are triggered by launching or stopping the model. They have been studied in the HSVA towing tank by accelerating and decelerating the model in various ways and in the B20 catapult facility by varying the location of the observation plane [3]. Former tests made by DLR in the WSG research-type small-size towing tank confirmed such effects and identified effects on vortex core structure (core size, velocity peak) and on circulation evolution [1].

It appeared also that temperature stratification could be a limiting factor for towing tank investigations characterised by specific values of the Brunt-Vaïsälä N^* frequency (a parameter linked to temperature gradient and vortex spacing b_0) [3,19]. It has an important effect on lateral vortex spacing and strength, the intensity of which was in rather good agreement with CFD predictions performed by CERFACS at comparable values of N^*.

For investigations of high-lift wing configurations at landing conditions (C_L~*1.4*) and without any stratification and end-effects disturbance, the validation domain could reasonably be identified as *~150b* and *~100b* for the HSVA towing tank and B20 catapult facility, respectively; ground effects usually alter the wake development behind these upper limits [3]. Thus, the combination of the afore-mentioned tools (wind tunnel/towing tank/catapult) is well suited for wake vortex identification in the near- to mid-/far-wake field. Specific instrumentation has been adapted or developed in some facilities to fully track wake vortices and to allow then evaluation of wake vortex minimisation candidates in these facilities [3,24].

2.3 Numerical simulations

Numerical simulations have also advanced significantly, resulting notably from work in the two last EC projects devoted to wake vortex characterisation and control (C-Wake and AWIATOR). Figure 4 identifies the different methods that can be used depending upon the Region of wake flow field (cf. § 2.1).

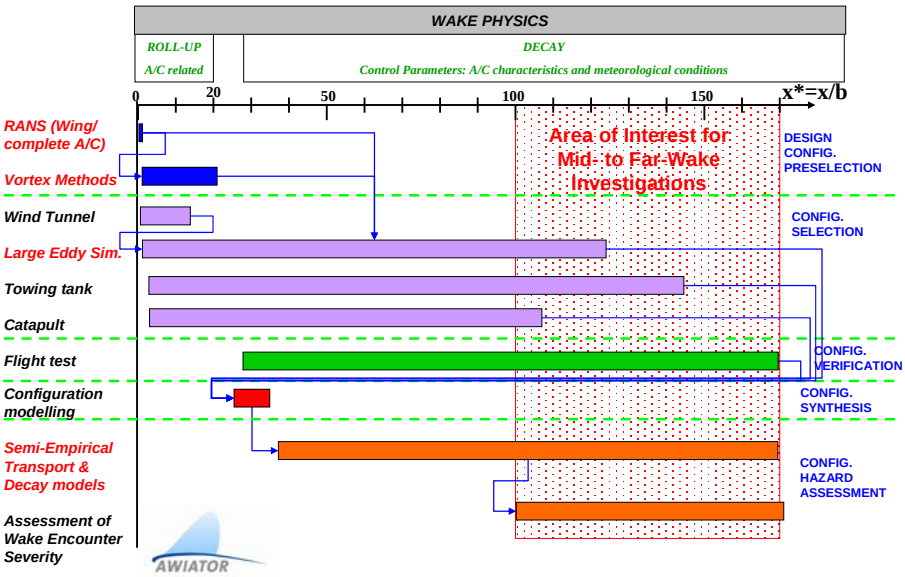

Figure 4 – Illustration of the Wake Characterization Prediction/Verification Methodology [24].

As Euler computations were applied to former test cases [8,29], it is now possible to do 3D RANS computations on a complete high-lift wing configuration down to 0.5 spans for both sub- and flight-scaled Reynolds numbers with different turbulence models [13,41]. Vortex methods [30,31] are very powerful and efficient to calculate the roll-up and vortex interactions from there on and should be considered in that respect. And further downstream, the interaction between the vortices and/or with atmospheric turbulence can be calculated with Large Eddy Simulation techniques ("LES") like the Vortex-In-Cell ("VIC") (results will be shown later in Fig. 16). A detailed comparison of various LES methods [12,13], the so called "bench mark study" done in the framework of the AWIATOR programme, clearly

indicated the maturity of these techniques. However, their "potential" limitations (2D/3D temporal, 3D spatial, input conditions, numerical schemes…) were clearly identified too [24].

It is to be noted that the initial conditions for vortex methods and LES simulations are very often obtained from smoothed experimental results to compute the wake flow subsequently up till ~120-150 spans. First attempts to create a "numerical chain" are under investigation at DLR and ONERA by coupling RANS (DLR code) to LES (ONERA code) simulations. The validation will be carried out, at first, on the reference high-lift wing configuration of the AWIATOR programme and could then be applied for wake vortex minimisation. Great care is required to mesh convergence, artificial viscosity effects as well as to RANS data transfer for LES initialisation at a given wake plane, downstream of the fuselage end. Figure 5 provides an example of wake data obtained by DLR [41] that will be used as input to LES simulations.

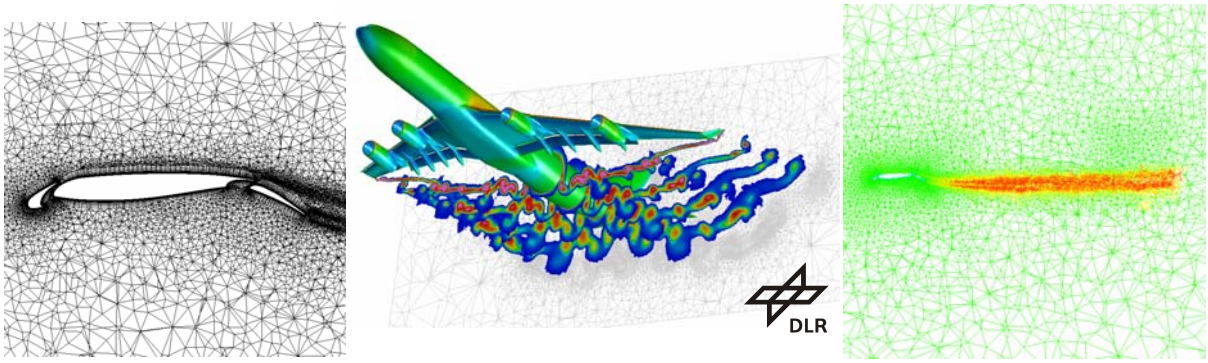

Figure 5 – Example of RANS data obtained for a high-lift wing configuration (AWIATOR, [41]).

Finally, the stability of vortex systems has been investigated with linear stability theory. Since the vortex distance b_0 is much larger than the vortex core, linear stability theory could also be applied successfully for a set (two, four or even six) of parallel vortex filaments with weak sinusoidal perturbations of their spatial positions. This allowed a parametric investigation in search for the highest levels of amplification for several multiple-vortex systems [15,16,22].

Thus, nowadays, a complete methodology/chain could be defined with support from theory, CFD, sub-scale tests and full-scale flight tests (cf. Fig. 4). It was recently validated for the wake characterisation of a baseline high-lift wing aircraft configuration (AWIATOR project, [24,28]). One can expect that this methodology can be employed in the future for the assessment of the wake alleviation potential of modified wing configurations.

3 WAKE VORTEX ALLEVIATION: TWO MAIN STRATEGIES

Knowing that it is impossible to inhibit the generation of the aircraft wake vortices [27,40], the question that has then to be considered is: “How can we alleviate, destroy wake vortices, or at least minimise their intensity”?

Two main strategies can be pursued for wake vortex alleviation:

- to act at the source, in the near-field, by either promoting small scale instabilities and increasing diffusion of vorticity or by introducing new turbulence in the vortex core, resulting in a larger but less intense core (reduction of peak velocity). The total circulation will not be affected, but a weaker rolling moment is expected for the following aircraft. This can be obtained by devices such as wing-tip, flap-tip ones, fences, spoilers…
- to create in the far-field a multiple-vortex system to promote long-wave instabilities and/or to trigger perturbations to obtain a premature wake collapse. This can be reached either by a passive concept leading to spanwise wing loading modification (via arrangement of flap or spoiler deflections) or by active devices such as blowing, oscillating flaps, ailerons…

Passive systems exploit the natural evolution of the instabilities modes with the highest growth rates, while active systems rely on hastening selected modes of instabilities by "forcing" the vortices. Both can be done using an existing vortex topology or by changing the vortex topology through a modification of the span load.

Vortices are characterised by a high degree of unsteadiness (Fig. 6); several experimental tests allowed identifying the presence of both short-wave (wavelength $\lambda \sim O(r_c)$ with r_c, core radius) and long-wave ($\lambda \sim O(b_0)$) instabilities [25,39]. The former (of Widnall-type) controls the merging of co-rotating vortex systems and could be enhanced for aircraft applications for wing-tip/flap-tip interactions. However, it would be unable to break down the wake vortex because of its weak dynamics when compared to the dominating mechanism of the rolling-up and evolution process of the wake vortices. The "classical" Crow instability ($\lambda \sim 8 b_0$) is able to destroy a pair of two counter rotating vortices, but its effectiveness is not obvious because of its low growth rate ($\sim 0.8\ \Gamma_0/(2\ \pi\ b_0^2)$) [7]. Crow himself proposed a forcing scheme using the control surfaces of a wing to hasten the development of cooperative instabilities of the vortex pair in its wake. This concept was checked in towing tank tests as well, but the development of the vortices was not long enough to check its efficiency (in [27]).

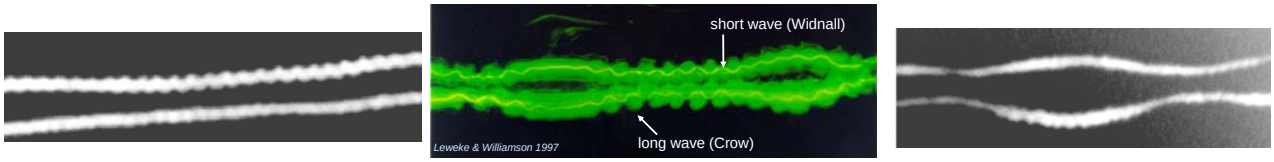

Figure 6 – Illustration of evidenced of short-wave and long-wave instabilities [2,25].

Instabilities are much more powerful for multiple vortex system. This can be realised by a modification of the wing span loading (either producing additional co- or counter rotating vortex pairs) possibly enhanced by Horizontal Tail Plane (H.T.P.), normally providing negative loading and hence a counter rotating vortex pair. The counter rotating vortices can produce medium-wave instabilities ($\lambda \sim O(b_0)$ referred to as "Omega Ω-loops") that are very fast growing and lead to strong interaction between vortices and generation of small scales and turbulence. As a result the vortex will be very much diffused. Consequently, the 2nd strategy is based on the notion that fast growing instabilities can amplify downstream and lead to the efficient destruction of the wake system. Thus, the two strategies represent different

concepts that might change the local or the global characteristics of the vortex system. Local modifications are obtained by adding specific devices to the wing whereas span load changes can be obtained from Differential Flap Setting ("D.F.S.") or Differential Spoiler Settings ("D.S.S."). These concepts will be discussed more in the following sections.

4 WAKE VORTEX ALLEVIATION: WHAT HAS BEEN ACHIEVED SO FAR

Devices, concepts or mechanisms for wake vortex alleviation have been studied in the past years from extensive sub-scale tests (using the combination of wind tunnels, towing tank and catapult facilities), from a few full-scale tests and from either CFD simulations or theoretical approaches. When available, all these different aspects will be evoked in the following discussions when dealing with i) wing add-on devices; ii) modification of spanwise wing loading, and iii) active wake control (through either active surface or blowing).

4.1 Wing add-on devices

In the framework of the C-Wake project wind tunnel tests were first conducted with devices to achieve near-field control like: wing tip and flap tip modifications, flaplet, turbulence generator, wish-bone and spoilers (Fig. 7) [8]. Results pointed out that in the near wake region for $x^*<5$, reduction of peak vorticity and maximum cross-flow velocity could be achieved, in combination with an enlargement of the vortex core [2,5,33,41]. Generally speaking, spread of the vorticity could be obtained, while the circulation of the controlled vortex remained unchanged. Some tests revealed that a rather strong re-distribution of the vorticity with wing tip and flap tip modifications at $x^*=1$ did not have any effect at $x^*=5$ [8].

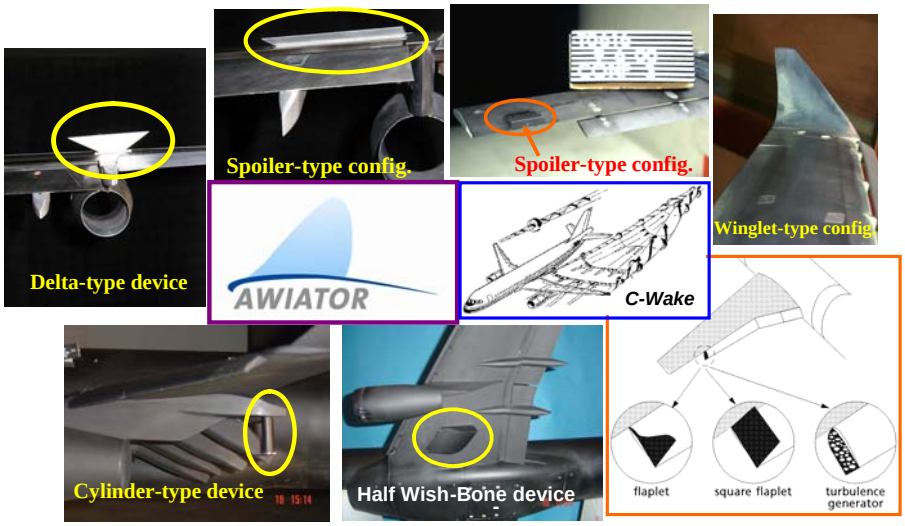

Figure 7 – Illustration of Wing add-on devices (C-Wake & AWIATOR projects).

Detailed investigations have been carried out later in the framework of the AWIATOR project in two wind tunnels, the HSVA towing tank and the B20 catapult, for three specific

devices suggested by Airbus Deutschland, Airbus France and DLR partners. One device consisted of a cylinder-type device, installed under the pylon extension fairing of the outboard nacelle (Fig. 7, bottom-left), aiming at injecting periodic perturbations into the flap vortex to enhance the instability of the four-vortex system generated from the outer edges of the flap and wing tips. Hot-wire measurements were made by TUM-AER in their wind tunnel using this device, and verified that the expected frequency emitted in the wake of the cylinder (for Strouhal number ~0.2) could be recorded very close to the device. However, from a power spectra analysis, this frequency could not be seen anymore at 4.5 spans behind the model, indicating that this device could not alter significantly the wake.

Another device, referred to as the "half wish-bone" device (cf. Fig 7, middle-bottom), was installed in between the inboard nacelle and the fuselage, on the pressure side of the wing. The generated counter-rotating vortex (w.r.t. wing tip vortex) could be identified close to the flap gap vortex, with comparable strength; however, measurements at the DNW-NWB wind tunnel with a 5-hole probe at $x^*=1$ [41] or at the catapult facility with PIV at $x^*=1.3$, 4.5 [3,24] could only detect the large momentum deficit it caused. Although the vortex of this device can possibly be combined with the horizontal tail-plane vortex, the half wish-bone as a stand-alone vortex generator was rather ineffective.

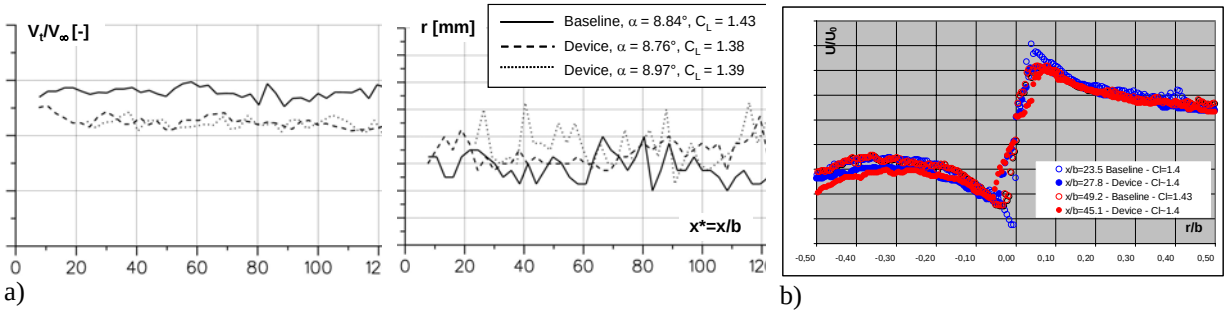

Figure 8. – Characterisation of wing add-on device (delta-type plate): a) peak vortex velocity and core radius (HSVA towing tank, PIV meas. [24]); b) tangential velocity profiles (B20 Catapult, Lidar measurements [3,24]).

Finally, a device will be discussed that looked like an inclined delta-type wing, installed at a spanwise location corresponding to that of the outboard nacelle, in the upper side of the wing trailing edge (cf. Fig. 7, upper left). Former tests, performed at HSVA and INSEAN towing tanks, provided encouraging results [8,20]. More recent investigations at the HSVA towing tank pointed out larger vortex cores, r_c, compared to the baseline configuration with a substantial reduction in the vortex spacing and in the peak vortex velocities, V_t/V_∞ (Fig. 8a, [24]). Complementary tests, at the ONERA B20 catapult, with the same device mounted on the free-flight model at almost similar high-lift configuration, confirmed the above-cited observations (Fig. 8b, [3,24]). The change in vortex spacing does suggest that this device also acted to shift the wing load more inboard.

Some specific winglet-type devices, either standard or larger ones, were also investigated; to see how the wing tip device (size) might affect the wake turbulence. The effect of a standard winglet on the wake flow is rather important, of course, in the vicinity of the wing

tip. However, several wind tunnel tests confirmed that at about one span behind the model, the effect on the iso-contours of the axial component of vorticity as well as on turbulent kinetic energy was within the experimental uncertainty [4]. At last, tests performed at HSVA towing tank with "large-sized" winglets (~3 times the dimensions of a "standard" one), applied to a large-transport aircraft type model, showed negligible effect on vortex sink speed, vortex separation distance, maximum tangential velocity or vortex core size.

There are unfortunately no CFD results for wing add-on devices for wake vortex control, partly due to the complexity of the calculations though some applications were reported for flap tip vortex manipulation with passive flaplets [8], partly related to noise assessments and concentrating only on the immediate near-wake flow field.

Finally, few computations (mainly Euler-type) and experiments demonstrated that the wake structure could be modified significantly in a region where vortex and engine jets are present [8]. Such work will be pursued in the Far-Wake project and will provide a systematic insight into the interactions of a wake vortex with either a cold or a hot jet flow.

4.2 Modification of spanwise wing load distribution: theoretical considerations.

This concept has got much attention in Europe for the last years [4,5,14,29], though it was investigated in the US in the 1970s. It was first evaluated experimentally by ONERA and DLR in the framework of the European C-Wake project [8], as part of their collaborative research programme [5], but also by ONERA under national research activities [4]. The European AWIATOR project provided the means to go in more detail using both theoretical and numerical approaches prior to and/or parallel to testing campaigns.

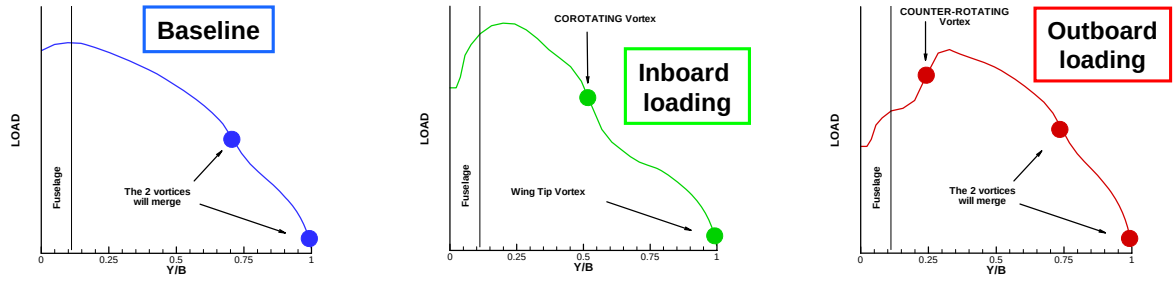

Figure 9 – Possible modifications of wing span load distribution ([38]).

The basic idea is to enhance instabilities by creating multiple-vortex system. For a specific span load distribution $\Gamma(y)$, Betz theory states that i) vortices are created at the maximum of the absolute value of the derivative of $\Gamma(y)$, ii) the vortex strength is proportional to the area between two local extremes to the 2nd derivative of $\Gamma(y)$. Hence, by changing the load distribution, e.g. by flap deflection, multiple vortex systems can be generated in principle. Normally, for a high lift wing configuration (the baseline configuration), two main (co-rotating) vortices originate from the outer flap tip and wing tip (Fig. 9, left) that merge very quickly, within a couple of spans behind the model. ONERA did calculate the baseline load

distribution and its variation for specific flap arrangements using 2D viscous computations on high-lift wing sections, combined with a 3D lifting surface [38]. The aim was to promote a strong inboard vortex, either co-rotating or counter-rotating relative to the combined outer flap / wing tip vortex (Fig. 9, middle and right, respectively). Illustrations of recorded wing span loading modifications as well as their effects in the wake flow field will be detailed later on, for large aircraft-type models (cf. Fig. 13).

Subsequently, UCL performed roll-up computations using a vortex method (AWIATOR project, [31,36]) starting from initial conditions taken from available data either from wind tunnel tests (using a rather fine grid resolution as in Fig. 13d) or from predicted lift distribution provided by ONERA (such as Fig. 13a). These calculations showed the evolution of the vortices and their final, double vortex pair, topology (Fig. 13e).

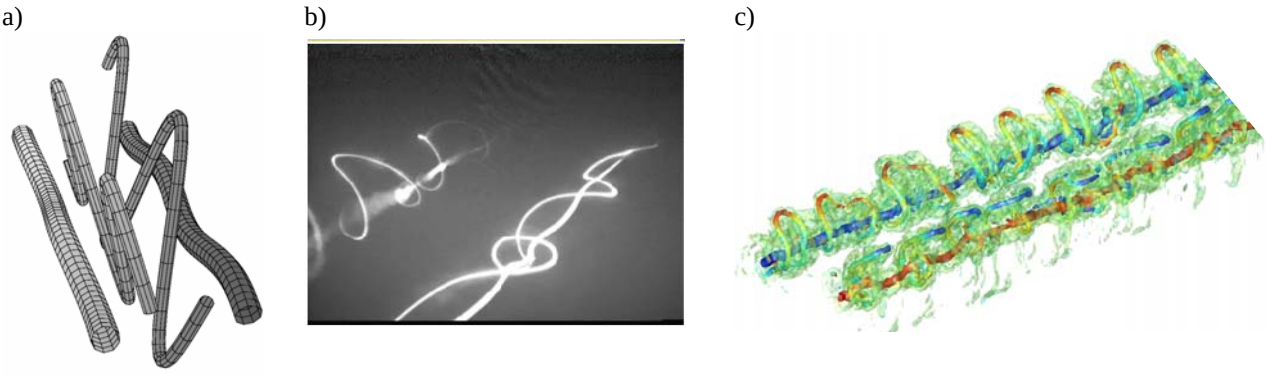

Figure 10 – Long wave perturbation in the wake of a 4-vortex system: a) linear stability theory [22]; b) Experiments [26]; c) iso-contours of vorticity at $\tau^*=0.48$ for LES [30,31,36].

Stability theory could be applied subsequently, starting from such a multiple vortex system. It was shown that a configuration with two vortex pairs of opposite sign (counter-rotating vortices) leads to much higher amplification rates than the "usual" Crow instability for a single vortex pair [15,16,22]. Figure 10a provides some result of the linear theory for $\Gamma_i/\Gamma_o=-0.3$ (ratio of the circulations of the inner vortex to the outer one) and $b_i/b_o=0.30$ (ratio of the corresponding vortex spacings). The most amplified perturbation (over all wave numbers) was plotted after one revolution of the inner vortices around the outer ones; it was amplified by a factor three orders of magnitude greater than that of Crow instability [22]. These calculations confirmed available towing tank results on very generic configurations [1,26,27,37] for comparable values of Γ_i/Γ_o (-0.37) and b_i/b_o (0.5) (Fig. 10b). Since stability theory is restricted to linear perturbations, the observed highly non-linear character of the interaction could not be calculated. But 3D vortex filament simulations by UCL [30,31,36] were able to capture the non-linear dynamics up to and beyond the time of strong interaction between vortices as well (Fig. 10c).

UCL made also many 3D LES simulations to further investigate instabilities and decay of counter-rotating four-vortex systems, taking into account the influence of different initial perturbations and the effect of spatial resolution [30,36]. Their parametric investigation

pointed out that a counter-rotating four-vortex system could significantly enhance vortex decay for appropriate ratios of circulation and spacing between vortices. The simulations visualised strong interactions between the counter rotating and the main vortices [36], with partial reconnection leading to fast generation of small scales, vortex bursting waves and turbulence. The so called "Ω-loops", which develop on the secondary vortices, interact strongly with the primary vortices, resulting in increased dissipation (up to 80 % of the initial kinetic energy) due the generated small scale turbulence and eventually vorticity exchange through the mid-plane. Depending upon the configuration, one could observe that the remaining weak vortices were embedded in a relatively strong turbulence field.

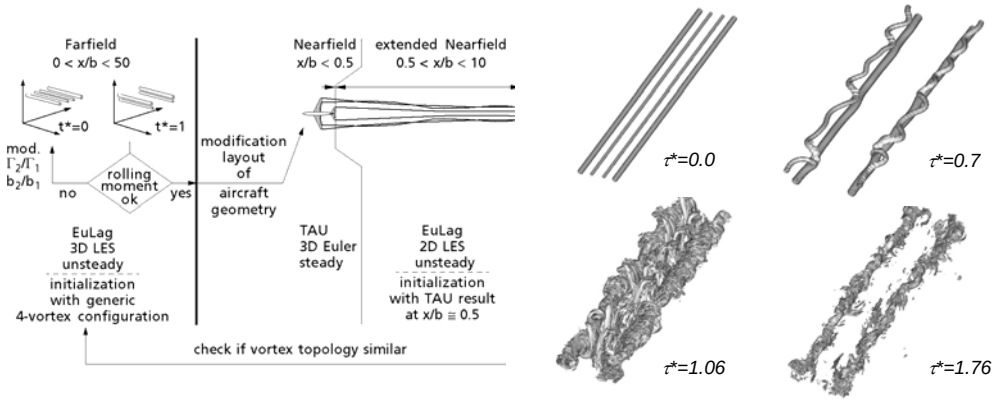

Figure 11 - Strategy for effective 4-vortex determination - left): numerical strategy; right): temporal development of iso-surfaces of vorticity for a given configuration [29].

A strategy for the optimization of 4-vortex systems to alleviate the wake vortex hazard was also described by DLR [29] based on the coupling of Euler and LES codes (Fig. 11, left). Once the parameters of the 4-vortex configuration, optimised for reducing rolling moment, are determined, the configuration of the considered aircraft is modified. This could be verified with a steady Euler-simulation for the modified aircraft configuration. The outcome of temporal LES simulation was displayed as iso-contours of the vorticity up to $\tau^*=1.76$ (Fig. 11, right). A significant decrease of rolling moment was calculated up to ~50% of the maximum rolling moment of a "standard" 2-vortex system. For this candidate 4-vortex system, the horizontal tail plane deflection was set such that it produced strong counter-rotating vortices

4.3 Examples of wing load modifications on models

Figure 12 illustrates some of the aircraft models that were used in the C-Wake and AWIATOR programs. For realistic aircraft configurations spanwise wing loading modifications could be obtained by specific flap arrangements. This is usually referred to as "D.F.S." or Differential Flap Setting. Thus, inboard wing loading is obtained with larger deflection angles of the inboard flap than of the outboard flap, and vice-versa for the outboard wing loading.

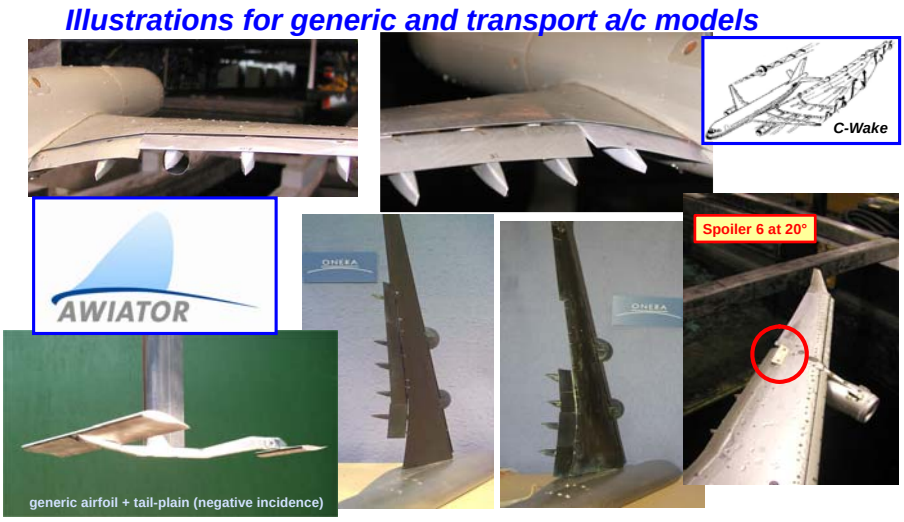

Figure 12 – Illustration of Differential Flap Setting "D.F.S." concepts for 2- and 3-flaps high lift systems, and generic airfoil for generating four-vortex system.

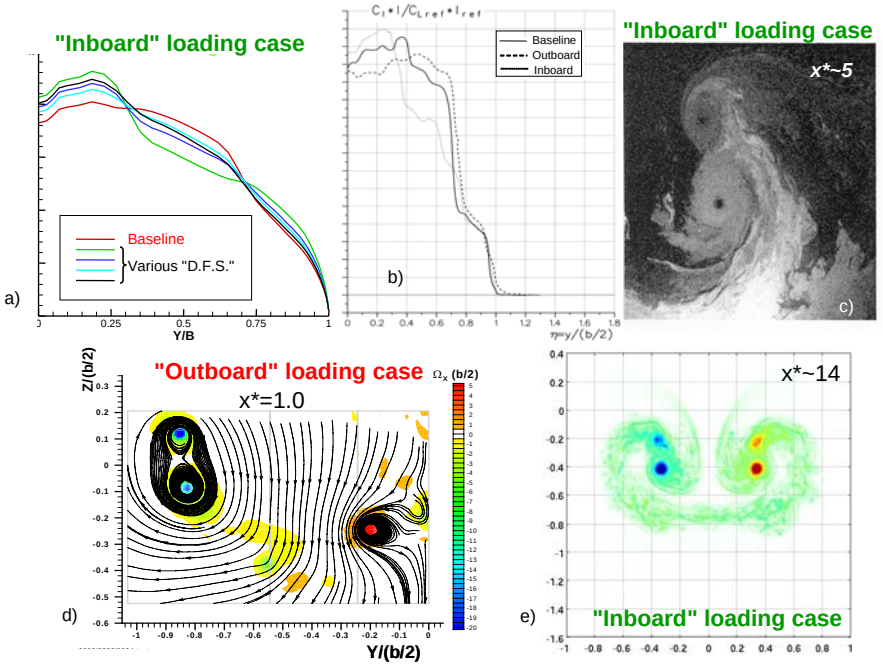

Figure 13 – Spanwise wing loading modifications for "Large transport aircraft-type model: a) computed load distribution [38]; b) load distribution deduced from measurements in the near-wake [24]; c) tomoscopy of the wake flow field [4]; d) measured wake flow field at x*=1 [5,38]; e) computed wake flow field at x*~14 [30,31].

This concept was applied to two high-lift wing configurations with either two or three flaps. From numerical and theoretical investigations as discussed above, inboard and outboard wing loading configurations were defined and subsequently tested both in the B20 catapult

and HSVA large towing tank facilities (AWIATOR project) [24]. A synthesis of towing tank tests results will be discussed below in relation with the Figures 14 & 15 [3,24].

DLR employed more generic-type models [1], similar to investigations made in the US [27,37]. Several horizontal tail planes (different chord lengths and spans) were tested in the DLR WSG towing tank to generate a vortex that interacts with the tip vortex of a rectangular wing (Fig. 12, bottom-left). This study showed that the interaction of counter-rotating tail vortices with tip vortices resulted in a promising self-destructive mechanism within the wake system similar to what was found in the calculation discussed above [1].

Figure 13 illustrates the modification on the load distribution, as well as the impact on the topology of the wake flow. In Figure 13a the load distributions as calculated by ONERA are shown for some typical D.F.S. configurations tested in the AWIATOR program. From wake surveys in the NWB wind tunnel of the DNW at $x^*=0.5$, it is possible to derive the spanwise wing loading (Fig. 13b) which looks very similar to the computed ones. Figure 13e gives a typical result of the vortex method as applied by UCL in the roll-up calculations showing a double pair of co-rotating vortices probably on its way to a final merger. Typical flow measurements evidenced too the multiple vortex system, depending upon the loading case (Figures 13c and 13d).

Some results for inboard loaded wings

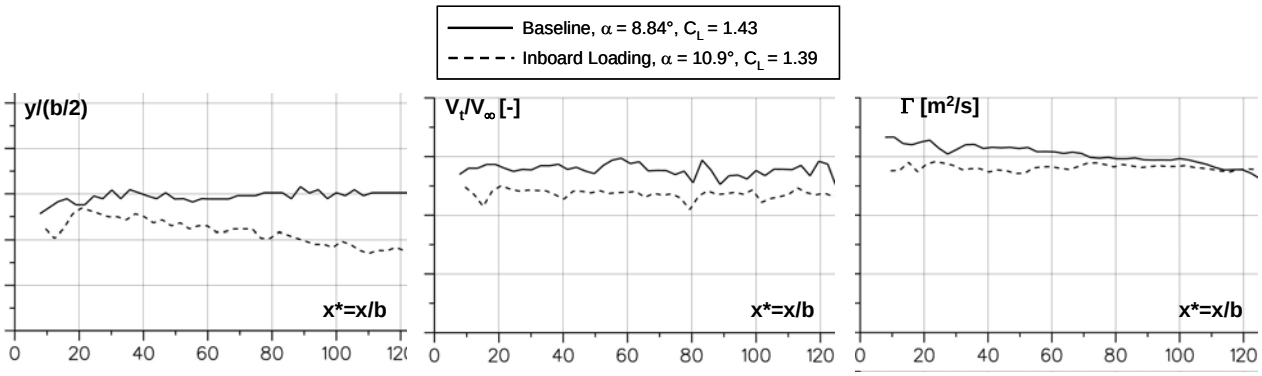

Figure 14 – Towing tank PIV results for inboard loading case on vortex spacing, peak velocity and circulation [24].

For inboard loading cases, tomoscopy applied at the ONERA B10 catapult facility clearly identified two co-rotating vortices per each half-plane at $x^*=5$ (Fig. 13c). This four-vortex system subsisted till ~25 spans, where it merged into a single vortex pair, more closely spaced, provoking then a steeper vortex descent [4] and (theoretically) a faster decay.

For the inboard loading case, HSVA towing tank measurements confirmed a significant reduction of the vortex spacing and a faster sink speed. In addition, a reduction of the maximal circumferential velocity, $V_{t,max}$., and an increase of the core radius ("fatter" vortex) were observed (Fig. 14). This latter point was also confirmed from catapult tests when plotting the tangential velocity profiles (Fig. 15, bottom-right). The evaluated circulation strength, $\Gamma_{5\text{-}15}$, was lower than the baseline case, the decrease being greater than that recorded from the catapult tests.

These results seem to suggest that the 4-vortex system does not exist for a sufficiently long time to enable the instabilities to develop and amplify to enhance the dissipation. Instead, the co-rotating vortices merge to establish a "conventional" vortex system, more closely spaced with a theoretically faster decay. It is also to be noted that instabilities, notably short wave instabilities, play a role in the merger of co-rotating vortices but this apparently doesn't lead to significantly increased dissipation. It remains to be seen if for other vortex topologies (e.g. a larger spacing for the two co-rotating vortices) the situation would have been different, or that merging would occur anyhow, though at larger distances. Nevertheless, the inboard loaded cases indicated some modest improvements relative to the base line.

Some results for outboard loaded wings

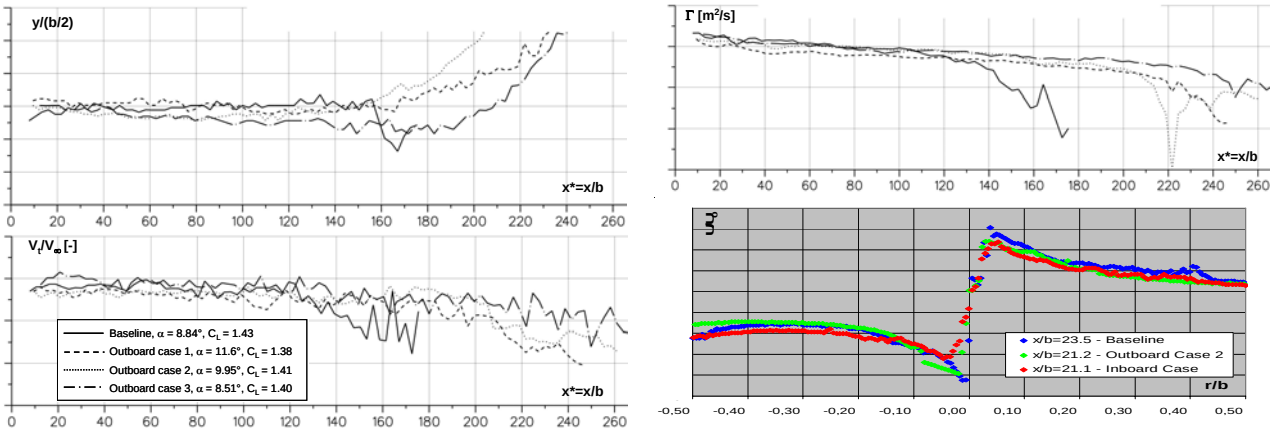

Figure 15 – Towing tank PIV results for outboard loading cases on vortex spacing, peak velocity and circulation ([24]) and catapult Lidar results on tangential velocity profiles for inboard and outboard loading cases ([38]).

Measurements, performed in the wind tunnel for the outboard loaded case at $x^*=1.0$ in a half-plane normal to the free-stream direction, revealed two intense counter-rotating vortices at a distance of about 1/4th of the half wing span (cf. Fig 13d, [4,5]). It appeared that the two visible vortices from the wing tip and outer flap tip (cf. same Fig. 13d), had merged rapidly at $x^*=2.25$. However, when tested in the mid-wake field in the B10 catapult facility, this multiple vortex system only lasted up till about 5 spans behind the wing, leading rapidly to a "conventional" vortex pair which went slower towards the ground, in agreement with the recorded increase in vortex spacing [4,5,8].

For similar outboard loaded configurations, the circulation strength $\Gamma_{5\text{-}15}$ as well as the maximum tangential velocity, $V_{t,max.}$, or the vortex core size, r_c, were almost the same as for the baseline configuration (Fig. 15). No significant advantage seemed to be offered. The catapult Lidar measurements confirmed that the effect on velocity profiles was smaller than that for the inboard loading case. Thus, apparently the generated inboard counter-rotating vortex is too weak, compared to the main vortex from the outer part of the wing (flap and wing tip) or is destroyed too rapidly, or has escaped, so that the generated multiple-vortex system could not sustain for too long and thus did not allow instabilities appearance.

4.4 Active control (through either active surfaces or blowing)

The idea is here to act “actively” in order to trigger the most powerful instabilities. Crouch et al. [6] successfully demonstrated in a towing tank an active control system to break up a four-vortex system, the wake of which comprised two co-rotating vortex pairs. The instability was forced by a symmetric excitation scheme of the control surfaces, preserving both total lift and aircraft symmetry.

Active surfaces

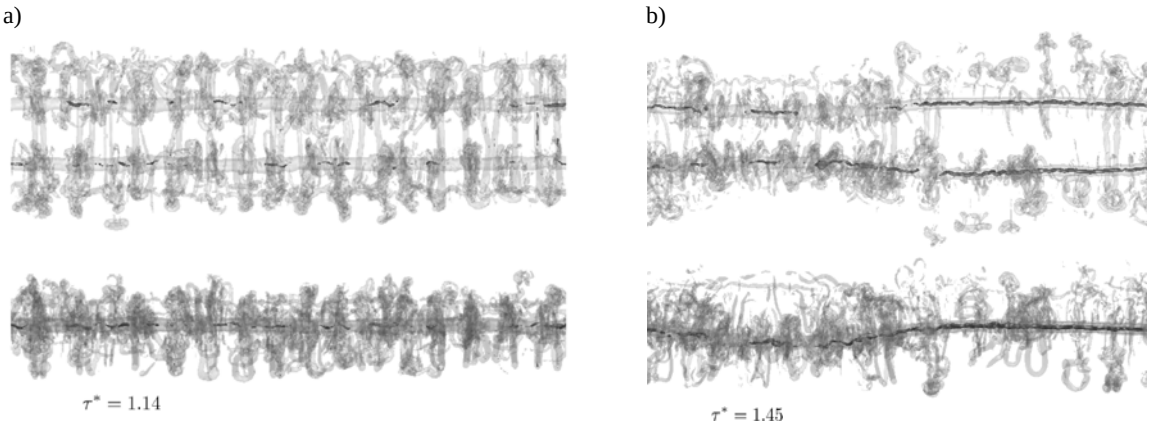

Figure 16 – Iso-vorticity surfaces from 3D LES simulations a) of the baseline configuration without oscillating ailerons at τ*=1.14 [13]; b) of the baseline configuration with oscillating ailerons at τ*=1.45 [30,31].

Temporal 3D LES simulations (over a large computational domain of about one oscillation cycle) were made recently by UCL to investigate the forcing of instabilities via periodic anti-phase inboard and outboard moving ailerons. They used the Vortex-In-Cell method combined with the parallel Fast Multi-Pole methods (“VIC-PFM”) [30,31]. Results plotted as iso-vorticity plots clearly demonstrated the growth of the Crow instability mode (Fig. 16b), the main vortices being substantially deformed, while the same plots for the reference configuration, at a comparable vortex life-time time, did not reveal such perturbation (Fig. 16a) [13]. Spectral analysis confirmed a large increase of the temporal evolution of the Crow instability mode.

DLR took also the opportunity of dedicated flight tests, in the framework of the AWIATOR project, to test some active control concept, using the ATTAS aircraft. The basic mechanism to introduce periodic disturbances into the flow field is a periodic alternation of the span-wise lift distribution, i.e. of the ratios of both the circulation and spacing of the distinct vortex pairs. In the flight tests Direct Lift Control ("DLC") flaps were used oscillating at a frequency corresponding to either long-wave length instability (Crow-type ~0.5Hz) or medium-wave length one (~2.1 Hz), the adjustment of the respective lift variation being made by the pilot. Weather issues (clouds) did not allow getting a full documentation of the tests. However, for the counter-rotating configuration it appeared to be possible to trigger the Crow instability, while perturbations made at both frequencies gave similar results.

Blowing devices

Another possibility of active control could be to blow in the vicinity of the outer part of a wing (outer flap, wing tip and aileron) to trigger instabilities to obtain a premature collapse of the wake vortex system. ONERA first worked with a simple counter-rotating topology, obtained from two half wings facing each other [34,35,39]. Continuous blowing at each wing-tip, in the free-stream direction at flow rate coefficients of about 1 10^{-3}, decreased noticeably the maximum level of vorticity and led to the disorganisation of the vorticity field [39] (Note that the flow rate coefficient is defined as $C\mu=\rho_b U^2_b S_b/\rho_0 U^2_0 S_0$, where indices *b* and *0* refer to blowing and free-stream conditions, respectively). Pulsed blowing at a frequency close to the Crow frequency (5.5Hz), but at a slightly higher flow rate (2.5 10^{-3}), decreased significantly the maximum vorticity [34,39].

ONERA investigated subsequently for a more complex initial wake topology (behind generic large transport a/c type model) the effect of continuous and pulsed blowing on the extended near-wake field. For the baseline configuration, several types of blowing were tested at the wing tip: axial, discrete holes or slots, and also at the external flap tip or in the aileron vicinity, at maximum flow rate coefficients of about 1 10^{-3} [4,34]. There was a minor effect on the maximum value of the axial vorticity component, while turbulent kinetic energy was increased in the vortex cores. At last, some pulsed blowing, using discrete holes, was applied. The pulsed frequency corresponded to the long-wave Crow instability that would be generated behind this model at such flow conditions (5Hz). At the furthest available downstream station ($x^*=2.25$), hot-wire measurements, in the vortex core and also outside, indicated that the unsteadiness was still present in the flow. This is rather encouraging since no unsteadiness was recorded at such vortex age for tests performed for instance with the wing add-on (cylinder-type) device as discussed before (cf. §4.1).

Further investigations will be devoted to the effect of blowing in the mid-wake field (at the ONERA catapult facility). Such study will raise challenging technological issues: pressurised tank as well as appropriate flow rates for the free-flight model.

5 WAKE VORTEX ALLEVIATION: CONCLUSIONS & RECOMMENDATIONS

The main features for wake vortex alleviation concepts have been discussed in the preceding sections. Some important features either understood or far from being understood, have been shown, and the main findings could be summarized as follows:

Wake physics, characterisation and simulation:

Thanks to the research in Europe, theoretical understanding, numerical simulation and measuring techniques have improved considerably over the last 10 years. The aircraft wake can be characterised in model experiments and in flight cases to sufficient detail. However, in the far field (at distances behind the aircraft roughly similar to the present day separation standards) the flow is very sensitive to weather effects (turbulence, stratification). Hence, a large data set is needed for wake characterisation in flight. Similarly, a large data set will be needed to validate ground based measurements (towing tank, catapult) with flight data.

Numerical simulations have advanced significantly, allowing looking into the details of the flow. The evaluation of the sensitivity of vortex roll-up, merging and evolution to mesh resolution, longitudinal domain extent, numerical scheme or initial perturbations still needs further investigations, yet. A full 3-D simulation of the wake of a real aircraft is still a too large problem. Several LES computations have started from test results or estimates provided by simplified methods; first attempts to couple LES to RANS methods are under development. Vortex filament methods in combination with stability theory could be applied systematically for a quick selection of interesting configurations for wake minimisation.

Wake vortex alleviation:

Research so far has not been very successful in reducing tremendously the wake vortex strength behind an aircraft. A weaker vortex can only result from design features that affect the decay characteristics far downstream. The most promising results have been obtained for the following devices or concepts (though some should be further investigated also with respect to the implications and applicability for a real aircraft):

- inboard loading: closer vortex spacing, giving more diffused and faster decaying vortex, was observed from computations and experimentally recorded.
- outboard loading configurations with multiple counter-rotating vortex pairs: enhanced dissipation due to violent non-linear vortex interactions was obtained numerically but was not detected from sub-scale tests.
- modification of wing span loading: substitution of differential flap settings by differential spoiler settings looked encouraging from sub-scale tests. Flight tests have to confirm this. Moreover, when considering outboard spoilers, significantly more diffused vortex were observed but the underlying causes were not clear.
- at last, for active control: moving flaps or ailerons, pulsed blowing could enhance instability modes like the Crow instability giving faster linking of the left and right vortex. Sub-scale tests are very difficult to handle correctly, notably for active control, and flight tests could help to state about their efficiency on wake vortex decay.

Acknowledgements The authors gratefully acknowledge Anton de Bruin (NLR), Abraham Elsenaar (former NLR), Florent Laporte (Airbus Deutschland), Stephan Melber-Wilkending (DLR) and Grégoire Winckelmans (UCL) for their valuable contributions to the present document.

REFERENCES

[1] Bao F., Vollmers H., Mattner H., 2003, *Experimental study on controlling wake vortex in towing tank*, Paper 8.3, in Proc. ICIASF Int. Congress on Instrumentation in Aerospace Simulation Facilities, Göttingen, Germany, 25-29 August 2003.

[2] Bristol R.L., Ortega J.M., Marcus P.S., Savas Ö, 2004, *Cooperative instabilities of a parallel vortex pair*, Journal of Fluid Mechanics, Vol. 517, pp. 331-358.

[3] Coustols E., 2005, *Testing in wind tunnels, towing tank and B20 Catapult,* AWIATOR Technical Workshop, Block II Experiments, Bremen, Germany 5-6 October.

[4] Coustols E., Jacquin L., Moens F., Molton P., 2004, *Status of ONERA research on wake vortex in the framework of national activities and European collaboration*, ECCOMAS 2004 Conference, Jyväskylä, Finland 24-28 July.
[5] Coustols E., Stumpf E., Jacquin L., Moens F., Vollmers H., Gerz T., 2003, *Minimised wake: a collaborative research programme on aircraft wake vortices*, AIAA Paper 2003-0938, 41st Aerospace Sciences Meeting & Exhibit Reno, NV, USA, 6-9 January 2003.
[6] Crouch J.D., Miller G.D., Spalart P.R., 2001, *Active control system for break-up of airplane trailing vortices*, AIAA Journal, Vol. 39, N°12, pp. 2374_2381.
[7] Crow S.C., 1970, *Stability theory for a pair of trailing vortices*, AIAA Journal, Vol. 8, N°12, pp. 2172-2179.
[8] C-Wake, 2003, *Wake Vortex Characterisation and Control*, Draft Final Report.
[9] de Bruin A.C., Winckelmans G., 2005, *Cross Cross-flow kinetic energy and core size growth of analytically defined wake vortex pairs*, NLR-CR-2005-412, AWIATOR Technical Report D 1.1.4-24, August.
[10] de Bruin A.C., Ganzevles F.L.A., 2003, *Drag and lift analysis from wake surveys at large distances behind a small aircraft model (SWIM model tests in DNW-LST wind tunnel)*, NLR-TR-2003-071, April.
[11] Desenfans O., Gigantelli S., 2004, *Instabilités des tourbillons de sillage d'aile avec décélération brusque : investigation dans le bassin de halage*, UCL, Internal Technical Report, Département de Mécanique.
[12] Dufresne L., Winckelmans G., 2005, *LES of the interaction and partial reconnection of unequal strength vortices*, Proc. Int. Conf. on high Reynolds number vortex interaction, ENSICA, Toulouse, France August 29-31.
[13] Dufresne L., Baumann R., Gerz T., Winckelmans G., Moet H., Capart R., Cocle R., Nybelen L., 2005, *Large Eddy simulation of wake vortex flows at very high Reynolds numbers: a comparison of different methodologies*, AWIATOR deliverable D1.1.4-16 ("Report on benchmark") August 2005; submitted to AS&T.
[14] Elsenaar, A., 2001, *The optimum wing load distribution to minimise wake vortex hazard*, Proc. Conf. on Capacity and Wake Vortices, London, 11-14 September 2001.
[15] Fabre D., Jacquin L., 2000, *Stability of a four-vortex aircraft wake model*, Physics of Fluids, Vol. 12, pp. 2438-2443.
[16] Fabre D., Jacquin L., Loof A., 2002, *Optimal perturbations in a 4-vortex aircraft wake in counter-rotating configuration*, J. Fluid Mech., Vol. 451, pp. 319-328.
[17] Gerz T., 2004, *Atmospheric impact upon the development of aircraft wake vortices*, ECCOMAS 2004 Conference, Jyväskylä, Finland 24-28 July.
[18] Gerz T., Holzäpfel F., Bryant W., Köpp F., Frech M., Tafferner A., Winckelmans G., 2005, *Research towards a wake vortex advisory system for optimal spacing*, C. R. Physique, Tome 6, Fascicule 4-5, pp. 501-523.
[19] Gerz T., Holzäpfel F., Darracq D., 2002, *Commercial aircraft wake vortices*, Progress in Aerospace Sciences, Vol. 38, pp. 181-208.
[20] Huenecke K., 2002, *Formation to decay: extended-time wake vortex characteristics of transport-type aircraft*, 20th AIAA Appl. Aero. Conf., St Louis, MO, June 24-27.
[21] Jacquin L., Fabre D., Geffroy P., Coustols E., 2001, *The properties of a transport aircraft wake in the extended near-wake field: an experimental study*, AIAA Paper 2001-1038, Reno Aero. Sci. Meet. and Exh., NV, USA, 5-8 January.
[22] Jacquin L., Fabre D., Sipp D., Coustols E., 2005, *Unsteadiness, instability and turbulence in trailing vortices*, C. R. Physique, Tome 6, Fascicule 4-5, pp. 399-414.

[23] Köpp F., Smalikho I., Rahm S., Dolfi A., Cariou J-P., Harris M., Young R.I., Weekes W., Gordon N., 2003, *Characterisation of aircraft wake vortices by multiple-lidar triangulation*, AIAA Journal, Vol. 41, pp. 1081-1088.
[24] Laporte F., 2005, *Aircraft configuration effects predicted by CFD and observed in experiments including F/T-1*, AWIATOR Technical Workshop, Block II Experiments, Bremen, Germany 5-6 October.
[25] Leweke T., Williamson C.H.K., 1996, *The long and short of vortex pair instability*, Physics of Fluids, Vol. 8, No. 9, September, pp. 55.
[26] Ortega J.M., Bristol R.L., Savas Ö, 2002, *Wake alleviation properties of triangular flapped wings,* AIAA Journal, Vol. 40, N°4, April, pp. 709-721.
[27] Savas Ö., 2005, *Experimental investigations on wake vortices and their alleviation,* C. R. Physique, Tome 6, Fascicule 4-5, pp. 415-429.
[28] Schrauf G., Laporte F., 2005, *AWIATOR Wake vortex characterization methodology*, Proc. CEAS/KATnet Conf. on Key Aerodynamic Technologies, Bremen, D, 20-22 June.
[29] Stumpf E., 2005, *Study of four-vortex aircraft wakes and layout of corresponding aircraft configurations*, Journal of Aircraft, Vol. 42, N°3, May-June, pp. 722-730 (also AIAA Paper 2004-1067, 42nd Aerospace Sciences Meeting and Exhibit, Reno, NV, USA, 5-8 January 2004).
[30] Winckelmans G., Cocle R., Dufresne L., Capart R., 2005, *Vortex methods and their application to trailing wake vortex simulations*, C. R. Physique, Tome 6, Fascicule 4-5, pp. 467-486.
[31] Winckelmans G., Cocle R., Dufresne L., Capart R., Bricteux L., Daeninck G., Lonfils T., Duponcheel, Desenfants O., Georges L., 2006, *Direct numerical simulation and large eddy simulation of wake vortices: going from laboratory conditions to flight conditions*, ECCOMAS CFD 2006, Egmond aan Zee, 5-8 september 2006.

Proceedings of the Workshop on "Principles of Wake Vortex Alleviation Devices" (ONERA Toulouse, 9-10 February 2006) that can be downloaded from the Web Site of the WakeNet2-Europe network at the following address:
http://wwwe.onecert.fr/projets/WakeNet2-Europe/wg7/public/programmeMeetingFebruary2005.htm.

[32] Bellastrada C., Breitsamter C., *Wake Vortex Alleviation by Means of Passive Vortex Devices*.
[33] Coustols E., *An overview of European projects on wake vortices*.
[34] Coustols E., Dor J-B., Jacquin L., Molton P., Moens F., Pailhas G., *Effect of continuous and pulsed blowing on the near- to mid-wake flow field generated behind a simple model and a generic aircraft-type model*.
[35] de Saint Victor X., *The ONERA Joint Project*, Meeting following the WakeNet2-Europe WG7 Workshop on "Wake Vortex Alleviation Devices", ONERA Toulouse.
[36] Dufresne L., Winckelmans G., Capart R., *LES of instabilities, vortex reconnection, and global decay of counter-rotating four vortex systems*.
[37] Durston R., *Wake vortex alleviation flow field studies*.
[38] Moens F., Dor J.B., Jacquin L., Molton P., Coustols E., *Effect of span-loading modification on the near- to mid-wake flow field*.
[39] Pailhas G., Touvet Y., Barricau P., *Instabilities developing in a wing tip counter rotating vortex pair: experimental evidence and control.*
[40] Savas Ö., *Passive Wake Vortex Alleviation*.
[41] Voss G., Stumpf E., *State of the current research on wake vortex alleviation*.